Lymphocyte Homing to Bronchus-associated Lymphoid Tissue (BALT) Is Mediated by L-selectin/PNAd, $\alpha_4\beta_1$ Integrin/VCAM-1, and LFA-1 Adhesion Pathways

Baohui Xu,[1,2,3] Norbert Wagner,[4] Linh Nguyen Pham,[1] Vincent Magno,[1] Zhongyan Shan,[1] Eugene C. Butcher,[1,2] and Sara A. Michie[1,2]

[1]*Department of Pathology, Stanford University School of Medicine, Stanford, CA 94305*
[2]*Pathology and Laboratory Medicine Service, Department of Veterans Affairs, Palo Alto Health Care System, Palo Alto, CA 94304*
[3]*Department of Environmental Medicine, Kagoshima University, Faculty of Medicine, Kagoshima 890-8520, Japan*
[4]*Department of Pediatrics, City Hospital of Dortmund, D-44137 Dortmund, Germany*

Abstract

Bronchus-associated lymphoid tissue (BALT) participates in airway immune responses. However, little is known about the lymphocyte–endothelial adhesion cascades that recruit lymphocytes from blood into BALT. We show that high endothelial venules (HEVs) in BALT express substantial levels of VCAM-1, in marked contrast to HEVs in other secondary lymphoid tissues. BALT HEVs also express the L-selectin ligand PNAd. Anti–L-selectin, anti-PNAd, and anti–LFA-1 mAbs almost completely block the homing of B and T lymphocytes into BALT, whereas anti–α_4 integrin and anti–VCAM-1 mAbs inhibit homing by nearly 40%. $\alpha_4\beta_7$ integrin and MAdCAM-1 are not involved. Importantly, we found that mAbs against α_4 integrin and VCAM-1 significantly block the migration of total T cells (80% memory phenotype) but not naive T and B cells to BALT. These results suggest that an adhesion cascade, which includes L-selectin/PNAd, $\alpha_4\beta_1$ integrin/VCAM-1, and LFA-1, targets specific lymphocyte subsets to BALT. This high level of involvement of $\alpha_4\beta_1$ integrin/VCAM-1 is unique among secondary lymphoid tissues, and may help unify lymphocyte migration pathways and immune responses in BALT and other bronchopulmonary tissues.

Key words: lung • bronchi • cell adhesion molecules • endothelium • CD106

Introduction

Lymphocyte migration from the bloodstream into secondary lymphoid tissues is mandatory for maintaining immune system homeostasis and providing efficient defense against pathogens (1). Much of this migration occurs through high endothelial venules (HEVs)* and is regulated in part by multistep cascades involving sequential lymphocyte/endothelial adhesion and activation events (2–5). These cascades differ from tissue to tissue, thus enabling certain subsets of lymphocytes to migrate efficiently into specific lymphoid tissues; this migration is partly controlled by tissue-selective expression of endothelial adhesion molecules that bind to ligands on circulating lymphocytes (6).

Bronchus-associated lymphoid tissue (BALT) consists of discrete lymphoid aggregates found in the bronchial mucosa in most mammals (7–9). Like other secondary lymphoid tissues such as lymph node (LN) and Peyer's patch (PP), BALT contains T cells, B cells, dendritic cells, macrophages, and HEVs (9). Because BALT and intestinal mucosa–associated PP show morphologic and functional similarities, both were thought to belong to a general mucosa-associated lymphoid system. For example, both BALT and PP provide for the entry of mucosal pathogens through special epithelial cells (M cells), and are involved in local IgA production (9). However, differences have been noted between BALT and PP. For example, in vitro lymphocyte/endothelial binding studies suggest that BALT and PP HEVs differ in their lymphocyte binding selectivity (10). Although BALT clearly plays a role in pulmonary immune

Address correspondence to Eugene C. Butcher, Dept. of Pathology, Stanford University School of Medicine, Stanford, CA 94305-5324. Phone: (650) 852-3369; Fax: (650) 858-3986; E-mail: ebutcher@stanford.edu

*Abbreviations used in this paper: BALT, bronchus-associated lymphoid tissue; CFSE, 5(6)-carboxyfluorescein diacetate succinimidyl ester; HEV, high endothelial venule; IF, immunofluorescence; LN, lymph node; MLN, mesenteric LN; NOD, nonobese diabetic; PLN, peripheral LN; PP, Peyer's patch; TRITC, tetramethylrhodamine-5-(and-6)-isothiocyanate mixed isomers; WT, wild-type.

 J. Exp. Med. © The Rockefeller University Press • 0022-1007/2003/05/1255/13 $8.00
Volume 197, Number 10, May 19, 2003 1255–1267
http://www.jem.org/cgi/doi/10.1084/jem.20010685

responses, the multistep cascade that controls the migration of lymphocytes to BALT, and the relationship of this cascade to the lymphocyte $\alpha_4\beta_1$/endothelial VCAM-1–dominant cascade involved in lymphocyte homing to pulmonary parenchyma, remain to be elucidated (11–15).

In this work, we explore the lymphocyte–endothelial adhesion pathways that control the migration of lymphocytes from the bloodstream into BALT. We show that BALT HEVs in nonobese diabetic (NOD), BALB/c, and C57BL/6 mice coordinately display PNAd and VCAM-1 at a level not found on HEVs in other secondary lymphoid tissues. Moreover, using adhesion-blocking mAbs in short-term in vivo lymphocyte homing assays, we find that L-selectin/PNAd, $\alpha_4\beta_1$/VCAM-1, and LFA-1 adhesion pathways are important in homing of specific lymphocyte subsets to mouse BALT. Our results suggest that this distinctive combination of adhesion receptors helps form a unique lymphocyte–endothelial cascade that is important in lymphocyte subset recruitment to BALT and in bronchopulmonary immune responses.

Materials and Methods

Animals. NOD, BALB/c, and C57BL/6 mice of both genders were purchased from Taconic or bred in our animal facility. Only nondiabetic NOD mice were used in this paper. Sprague Dawley rats and C57BL/6 Thy1.1 IgM^a mice were obtained from The Jackson Laboratory. C57BL/6 β_7 integrin KO (β_7 KO) mice are described previously (16). OVA TCR transgenic mice (DO11.10) were obtained from Drs. D. Loh and O. Kanagawa (Washington University, School of Medicine, St. Louis, MO), and The Jackson Laboratory. All animals were housed under specific pathogen-free conditions in the Palo Alto Veterans Affairs or Stanford University animal facilities.

Antibodies and Other Reagents. mAbs used in this paper were the following: anti-CD4 (GK1.5), anti-CD8 (53–6.7.2), anti-α_4 (PS/2), anti–LFA-1 (FD441.8), and anti–ICAM-1 (BE29 and YN1.7), grown from hybridomas obtained from the American Type Culture Collection; anti-$\alpha_4\beta_7$ integrin heterodimer (DATK32), anti-β_7 (FIB 504), anti–L-selectin (MEL-14), anti-PNAd (MECA79), and anti–MAdCAM-1 (MECA367), grown from hybridomas produced in our laboratory; anti-VCAM-1 (MK2.7, 4B12, 2A11.1 and 6C7.1, Dr. B. Engelhardt, Max Planck Institute, Munster, Germany); anti-CD45R/B220 (RA3–6B2, Dr. R. Coffman, DNAX Research Institute, Palo Alto, CA); anti-OVA TCR (KJ1–26, Dr. J. Kappler, National Jewish Medical and Research Center, Denver, CO); anti–P-selectin (RB40.34), anti–E-selectin (10E9.6), anti–ICAM-2 (3C4), anti-CD44 (IM7), anti-Thy1.1 (OX-7), and anti-IgM^a (DS-1), purchased from BD Biosciences; and anti-CD3 (KT3) from Accurate Chemical. Rat anti–human CD44 (9B5; our laboratory) and rat anti–mouse cerebellar antigen (OZ42; Dr. L. Pickford, Coulter Pharmaceutical, Menlo Park, CA) were used as negative control mAbs.

Biotin-anti–rat IgG, FITC-anti–rat IgG, and FITC-anti–rat IgM were purchased from Vector Laboratories. Biotin-anti–rat IgM and peroxidase-streptavidin were purchased from Jackson ImmunoResearch Laboratories, whereas PE-anti–rat IgG came from Biosource International. 3,3′-diaminobenzidine-tetrahydrochloride (DAB) was purchased from Sigma-Aldrich, while 5(6)-carboxyfluorescein diacetate succinimidyl ester (CFSE) mixed isomers, tetramethylrhodamine-5(6)-isothiocyanate mixed isomers (TRITC), and Alexa Fluor 488 were obtained from Molecular Probes.

Morphometric Analysis of BALT. Mice were killed, and the lungs filled with PBS/OCT (1:1) by intratracheal injection, removed, and frozen in OCT. Frozen sections of the left lung were stained with hematoxylin and eosin; slides that showed a longitudinal section of a main bronchus that extended for at least one half the length of the lung tissue were used for image analysis as described previously (VAS II; Video Systems; reference 17). In brief, we measured the area of all BALT aggregates and the bronchus on at least 20 nonsequential sections from each mouse. Results for each mouse are presented as the ratio of the BALT area (mm^2) to the bronchus area (mm^2).

Immunohistochemistry. Acetone-fixed frozen sections of lung, peripheral LN (PLN), and PP were sequentially incubated with hybridoma supernatant or purified mAb (1 h), biotin-anti–rat IgG or biotin-anti–rat IgM Ab (30 min), peroxidase-streptavidin (30 min), and DAB solution (10 min). The slides were washed in PBS after each incubation step. Some slides were counterstained with hematoxylin or methylene blue.

Evaluation of Vascular Luminal VCAM-1 Expression. 100 μg anti–VCAM-1 (4B12, 2A11.1, or 6C7.1) or negative control (9B5) mAb was given intravenously to NOD and BALB/c mice (8–15-mo-old). The mice were killed 3 min after injection and perfused immediately with PBS through the right ventricle. Frozen sections of lung, PLN, mesenteric LN (MLN), and PP were incubated sequentially with 2 μg/ml PE-anti–rat IgG, PBS, 10% normal rat serum, and Alexa 488–conjugated anti-PNAd, anti–MAdCAM-1, or control mAb (10 μg/ml). We examined the sections by confocal or immunofluorescence (IF) microscopy, and determined how many HEVs in BALT, PLN, and MLN expressed both PNAd and VCAM-1, only PNAd, or only VCAM-1. Similarly, we determined how many PP HEVs expressed both MAdCAM-1 and VCAM-1, only MAdCAM-1, or only VCAM-1.

T and B Cell Migration into BALT. 5×10^7 lymphocytes from LN and spleen of C57BL/6 Thy1.1 IgM^a mice were transferred intravenously into each NOD host mouse (Thy1.2, IgM^b; >8-mo old). Hosts were killed 2 h later; 10^6 lymphocytes from PLN, PP, MLN, spleen, and blood suspensions, as well as 10^6 donor lymphocytes used for the transfer (input cells), were incubated for 30 min at 4°C in 100 μl of 0.5 μg/ml PE–anti-Thy1.1 and 1 μg/ml FITC–anti-IgM^a or isotype- and conjugation-matched negative control mAbs. Two-color flow cytometry was used as described previously to determine the percentage of cells in the lymphocyte scatter gate that expressed Thy1.1 or IgM^a (18). At least 5×10^4 cells in the lymphocyte gate were analyzed on each sample. Frozen sections of host lungs stained with 2 μg/ml PE–anti-Thy1.1 and 4 μg/ml FITC-anti-IgM^a mAbs were evaluated by confocal microscopy; donor T and B cells in BALT were counted on >30 sections of lung from each mouse. Data are expressed as the ratio of donor T (Thy1.1$^+$)/donor B (IgM^{a+}) cells in each tissue divided by the Thy1.1$^+$/IgM^{a+} input ratio.

In Vivo Blocking of Lymphocyte Homing by Anti–adhesion Molecule mAbs. Lymphocytes from LN and spleen of 3–4-mo-old NOD mice were labeled by incubating 2×10^7 cells/ml with 0.8 μg/ml TRITC in labeling medium (50% RPMI 1640, 48.5% HBSS, and 1.5% BCS) at 37°C for 15 min (19). Similarly, rat LN and spleen lymphocytes were labeled with 4 μM CFSE as described previously for TRITC (20). The cells were centrifuged through BCS, washed, and resuspended in transfer medium (DMEM with 10 mM Hepes, and 1% BCS).

To block endothelial adhesion molecules, each host mouse received 500 μg intravenously of anti–endothelial adhesion molecule or control mAb, followed 30 min later by 5×10^7 TRITC-labeled mouse cells intravenously. To block lymphocyte adhesion molecules, TRITC-labeled mouse cells were treated with 10 μg/ml anti–lymphocyte adhesion molecule or control mAb on ice for 10 min; 5×10^7 mouse cells and 10^8 CFSE-labeled rat cells were transferred intravenously into each host. The rat cells, which do not react with the anti–mouse lymphocyte adhesion molecule mAbs used in these experiments, served as an internal standard to control for differences between host mice in blood flow to tissues and in the efficiency of the injection. An aliquot of the labeled mouse and rat cell mixture was used to obtain the input mouse/rat cell ratio. To ensure saturating mAb levels in vivo, additional mAb (100 μg anti–endothelial or 250 μg anti–lymphocyte adhesion molecule) was given along with the donor cells. In all experiments, host mice were killed 2 h after transfer. Staining with FITC-anti–rat IgG or IgM of tissues from host mice that received anti–VCAM-1 or anti-PNAd mAb, and staining of lymphocyte suspensions from host mice that were given anti–LFA-1 mAb-coated lymphocytes showed that mAb was present on mouse endothelia or lymphocytes, respectively, at the time of sacrifice (unpublished data).

In experiments involving blocking of endothelial adhesion molecules, flow cytometry was used to determine how many donor cells were in host blood and how many donor cells had migrated into host PLN, PP, MLN, and spleen. In brief, for each cell suspension, we determined the absolute number of donor cells ($TRITC^+$) and total cells in the lymphocyte scatter gate; at least 5×10^4 total gated cells were analyzed for each sample. We calculated donor cells as a percentage of total gated cells in each tissue. The donor cells in BALT were observed by confocal microscopy, and homed cell density was calculated as the number of donor cells/10^3 μm^2 of BALT. At least 30 sections of lung were evaluated per mouse. For each tissue, results for each specific mAb treatment are expressed as percent homing in control mAb-treated host mice.

In experiments involving blocking of lymphocyte adhesion molecules, the numbers of donor mouse ($TRITC^+$) and internal standard rat ($CFSE^+$) cells were evaluated in host PLN, PP, MLN, spleen, and blood by two-color flow cytometry and in BALT by confocal microscopy. The donor mouse/internal standard cell ratios for all tissues were normalized by the input mouse/internal standard cell ratio. For each tissue, results for each specific mAb treatment are expressed as percent homing of control mAb-treated cells.

In preliminary experiments, we compared data in PLN, PP, and MLN obtained by flow cytometry and confocal microscopy and confirmed that there is a good correlation between the two assays ($r = 0.97$; unpublished data).

Homing of Lymphocytes from β_7 KO Mice. LN and spleen lymphocytes from 3–4-mo-old C57BL/6 β_7 KO and C57BL/6 wild-type (WT) mice were labeled with TRITC and CFSE, respectively, and injected intravenously into NOD mice (5×10^7 of each cell type per mouse). Numbers of donor cells in PLN, PP, MLN, spleen, blood, and BALT were determined as described previously. The results are presented as the ratio of β_7 KO/WT lymphocytes in each tissue divided by the β_7 KO/WT input ratio.

Naive T Cell Homing. We prepared lymphocyte suspensions of LN and spleen from 6-wk-old DO11.10 OVA TCR transgenic mice and age-matched C57BL/6 Thy1.1 mice. The DO11.10 T cells have a naive phenotype, whereas the C57BL/6 Thy1.1 T cells, which are a mix of naive and memory cells, served as internal standards. 5×10^7 DO11.10 lymphocytes and an equal number of C57BL/6 Thy1.1 lymphocytes were transferred intravenously into each NOD mouse. 2 h later, mice were killed and lymphocyte suspensions from PLN, PP, MLN, spleen, and blood were stained with 2 μg/ml FITC-anti–OVA TCR (KJ1–26) and 0.5 μg/ml PE–anti-Thy1.1 mAbs; donor DO11.10 naive T cells (OVA TCR^+) and internal standard C57BL/6 T cells ($Thy1.1^+$) were detected by flow cytometry as described earlier in Materials and Methods. Frozen sections of lung stained with 4 μg/ml FITC-KJ1–26 and 2 μg/ml PE–anti-Thy1.1 mAbs were examined by confocal microscopy for DO11.10 and internal standard T cells in BALT. Data are expressed as the ratio of OVA TCR^+ (naive)/$Thy1.1^+$ (internal standard) T cells in BALT, PLN, PP, MLN, and blood normalized for their ratio in the spleen.

To evaluate the roles of PNAd, α_4, and VCAM-1 in the homing of total T cells, naive T cells, and B cells to BALT, 5×10^7 lymphocytes from 6-wk-old DO11.10 mice ($KJ1–26^+$ naive T cells, IgM^{a+} B cells) or 19-mo-old C57BL/6 Thy1.1 mice were transferred intravenously into NOD host mice; as described earlier in Materials and Methods, the host mice were treated with anti-PNAd or anti–VCAM-1 mAb, or the donor cells with anti-α_4 mAb, before the transfer. Host mice were killed and their lymphoid tissues were stained with a FITC-conjugated mAb against OVA TCR, IgM^a, or Thy 1.1, and evaluated as described earlier in Materials and Methods. The results for the specific mAb treatment are presented as percent homing of the control mAb treatment.

Data Analysis. Data are given as mean ± SE for each group. One-way analysis of variance (ANOVA) was used for statistical analysis unless otherwise indicated. $P < 0.05$ is considered to be statistically significant.

Results

BALT and Its Lymphocyte Subsets in NOD, BALB/c, and C57BL/6 Mice. To define the best mouse strains for the study of lymphocyte migration to BALT, we examined histologic sections of lungs from adult mice of several strains and ages (6 wk–2 yr). We found BALT in most old (>1 yr), but not young, BALB/c and C57BL/6 mice. In contrast, BALT was easily identified in most NOD mice, especially those older than 7 mo. Tissue section morphometry of lung sections from 1-yr-old NOD, BALB/c, and C57BL/6 mice showed that NOD mice had the most abundant BALT, with a BALT area (mm^2) to bronchus area (mm^2) ratio of 0.12 ± 0.02 (mean ± SE), followed by BALB/c mice (Fig. 1; 0.08 ± 0.02). C57BL/6 WT and C57BL/6 β_7 KO mice had the least BALT (0.05 ± 0.02 and 0.04 ± 0.01, respectively; $P < 0.05$, C57BL/6 KO compared with NOD and BALB/c). There were no differences in BALT area between female and male mice (unpublished data).

NOD BALT, like BALB/c and C57BL/6 BALT, was composed predominantly of small lymphocytes without germinal centers. We stained frozen sections of lungs from these mice with mAbs against B cells, T cells, and T cell subsets. In most BALT aggregates, B cells outnumbered T cells; most of the T cells were $CD4^+$ (Fig. 2). Prominent

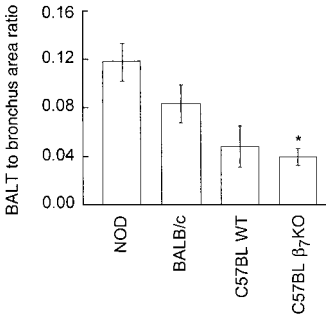

Figure 1. Prominence of BALT in various mouse strains. BALT and bronchial areas (mm^2) were determined by morphometric analysis of lung sections from 1-yr-old NOD ($n = 6$), BALB/c ($n = 5$), C57BL/6 WT ($n = 4$), and C57BL/6 β7 integrin KO ($n = 4$) mice. BALT was significantly more abundant in NOD and BALB/c mice than in C57BL/6 KO mice (*, $P < 0.05$ compared with NOD and BALB/c, Mann-Whitney test). Data for each group are given as mean ± SE.

HEVs were seen in BALT from all strains. Because NOD BALT is easily found, but shows similar histology and cellular composition to BALT from other strains, we used NOD mice as our main model to study the adhesion cascades that control lymphocyte migration to BALT.

T and B Cells Migrate from Blood into BALT. We initially compared the efficiency of homing of T versus B cells from the bloodstream into BALT. For this purpose, lymphocytes from C57BL/6 Thy1.1 IgM^a mice were transferred intravenously into NOD (Thy1.2, IgM^b) mice. Donor T and B cells in host lymphoid tissues and blood were detected by staining with PE–anti-Thy1.1 and FITC–anti-IgM^a mAbs, followed by flow cytometry or confocal microscopy. The relative abilities of T and B cells to migrate into each lymphoid tissue were determined by normalizing the T/B cell ratio in the tissue by the input T/B cell ratio. We found that T cells homed much more efficiently than B cells to BALT and PLN, with normalized T/B cell homing ratios of 3.3 for BALT and 6.6 for PLN (Fig. 3). T cells migrated slightly better than B cells to PP and MLN with normalized T/B cell ratios of 1.3 and 1.4, respectively. However, B cells migrated more efficiently than T cells to spleen with the ratio of 0.5. Thus, the pattern of T versus B cell recruitment by BALT seems intermediate between that of PLN and PP.

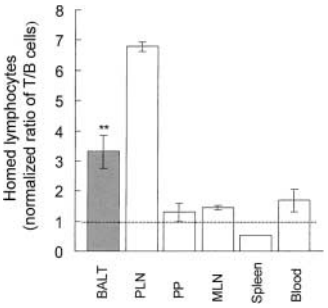

Figure 3. T and B cell migration to BALT. Lymphocytes from C57BL/6 $Thy1.1^+$ IgM^{a+} mice were transferred intravenously into NOD mice ($Thy1.2^+$ IgM^{b+}). Host lymphoid tissues and blood were stained with PE–anti-$Thy1.1^+$ (donor T cells) and FITC–anti-IgM^a (donor B cells) mAbs, followed by flow cytometry or confocal microscopy. Results are presented as the ratio of T to B cells migrating into each organ, normalized by dividing by the T / B cell input ratio (mean ± SE). Data from three hosts indicate that T cells migrate to BALT more efficiently than do B cells. (**, $P < 0.01$, BALT [gray bar] compared with PLN, PP, MLN, or spleen [white bars]).

Expression of Lymphocyte and Endothelial Adhesion Molecules in BALT. The functional and histologic similarities between BALT and PP, including the presence of HEVs, led us to hypothesize that lymphocytes home to BALT using lymphocyte–endothelial adhesion pathways similar to those used in PP and other secondary lymphoid tissues. To address this hypothesis, we stained frozen sections of BALT, PLN, and PP with mAbs against several lymphocyte and endothelial adhesion molecules that are involved in lymphocyte migration into secondary lymphoid tissues (1). These include the following: lymphocyte L-selectin and endothelial PNAd, which play a major role in migration of naive lymphocytes into PLN and a minor role in such migration into PP (3, 5, 21, 22); lymphocyte $\alpha_4\beta_7$ and endothelial MAdCAM-1, which mediate lymphocyte mi-

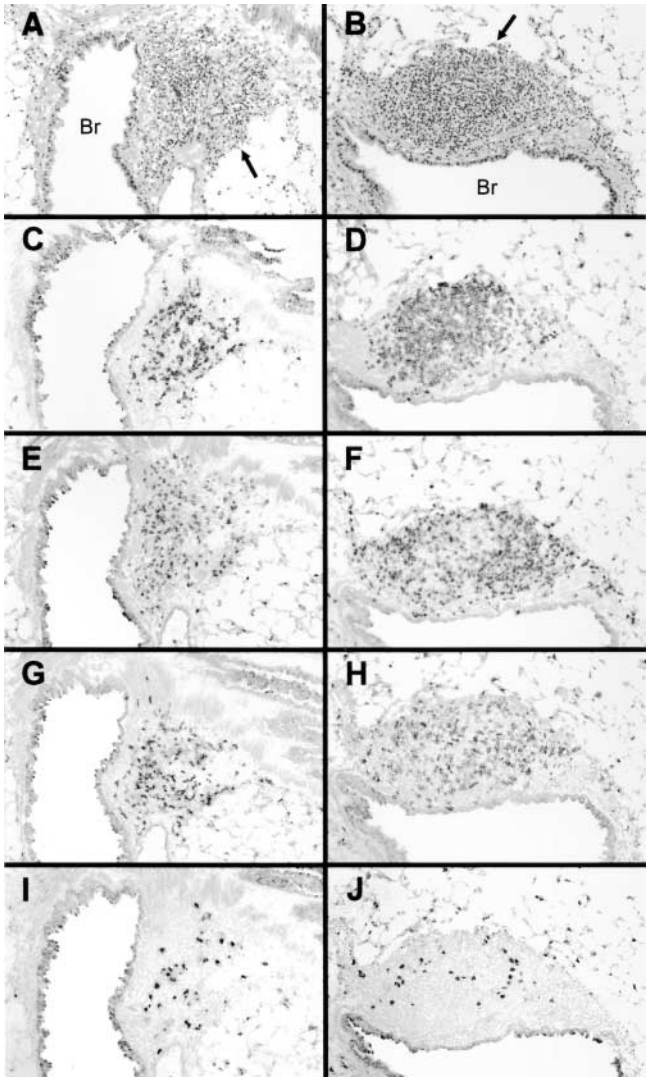

Figure 2. Lymphocyte subsets in BALT. Frozen sections of lung from NOD (A, C, E, G, and I), BALB/c (B, D, F, H, and J), and C57BL/6 (not depicted) mice were stained with hematoxylin and eosin (A and B), or anti-B220 (C and D), anti-CD3 (E and F), anti-CD4 (G and H), and anti-CD8 (I and J) mAbs. There was no staining using isotype control mAbs (not depicted). (Arrows indicate BALT; Br is in bronchial lumen; C–J, immunoperoxidase stains; original magnification = 20.)

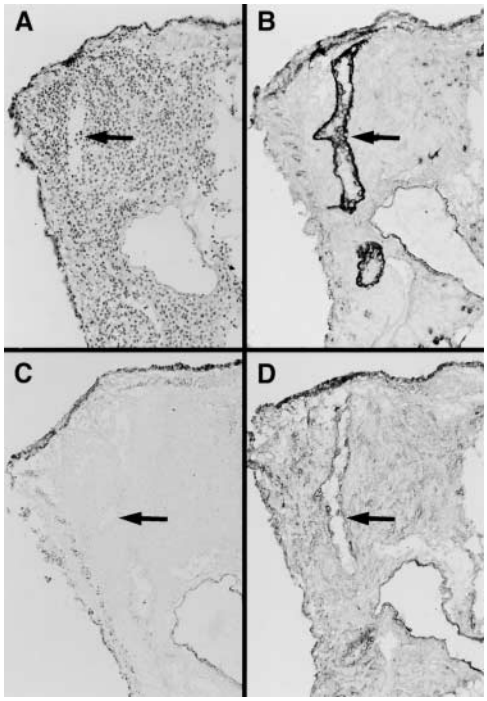

Figure 4. PNAd and VCAM-1, but not MAdCAM-1, are expressed by BALT HEVs. Serial frozen sections of lung from a 1-yr-old NOD mouse were stained with hematoxylin and eosin (A), or anti-PNAd (B), anti–MAdCAM-1 (C), and anti–VCAM-1 (D) mAbs. There was no staining using isotype control mAbs (not depicted). (Arrows indicate HEV; B–D, immunoperoxidase stains; original magnification = 20.)

gration into intestinal lymphoid tissues such as PP and lamina propria (3, 22, 23); and lymphocyte LFA-1 and endothelial ICAM-1, which are involved in lymphocyte migration into most secondary lymphoid tissues and sites of chronic inflammation (24–26). We also examined BALT for expression of adhesion molecules that mediate lymphocyte homing mainly to sites of chronic inflammation; these molecules include VCAM-1, which is expressed by endothelia in a wide variety of chronically-inflamed tissues, and its lymphocyte ligands $\alpha_4\beta_1$ and $\alpha_4\beta_7$ (11–15, 27–30).

Immunohistochemical stains showed that the patterns of endothelial adhesion molecule expression in NOD mice (Fig. 4) were identical to those in BALB/c and C57BL/6 mice (not depicted). Specifically, anti-PNAd mAb gave strong staining of HEVs in BALT (Fig. 4 B) and PLN, whereas weak staining was observed on HEVs in PP. Anti–MAdCAM-1 mAb gave no staining of HEVs in BALT (Fig. 4 C) and PLN, and strong staining of HEVs in PP. BALT HEVs stained strongly for ICAM-1 and ICAM-2 (not depicted). There was no staining of HEVs in BALT for E- or P-selectin, although there was strong staining of vessels in the positive control slide of inflamed tongue. There was no staining of BALT HEVs by isotype control mAbs.

Immunohistochemistry showed staining for VCAM-1 on BALT HEVs (Fig. 4 D), but no staining above background on PLN and PP HEVs (not depicted). However, previous papers indicate that VCAM-1 expression is not restricted to endothelia; it is expressed by a variety of cells and extracellular structures, including pericytes and connective tissues that form the perivascular sheaths surrounding some HEVs (31). Thus, to determine whether BALT HEVs display VCAM-1 on the endothelial luminal surface, where the VCAM-1 would be available to bind its lymphocyte ligands, we injected anti–VCAM-1 or negative control mAb intravenously into NOD and BALB/c mice (n = 5 mice of each strain). Mice were killed 3 min after injection, and sections were prepared from lung, PLN, MLN, and PP. These sections were stained with PE-anti–rat IgG (to detect injected mAb) and an Alexa 488–conjugated mAb against a vascular addressin (PNAd in BALT, PLN, and MLN; MAdCAM-1 in PP). Sections were ex-

Table I. *VCAM-1 Is Expressed on the Endothelial Luminal Surface of Almost all HEVs in BALT and on Rare HEVs in Other Secondary Lymphoid Tissues*

	NOD			BALB/c		
Tissue	Addressin only[a]	VCAM-1 only	Dual expression	Addressin only[a]	VCAM-1 only	Dual expression
	%	%	%	%	%	%
BALT	6.2 ± 1.1	2.6 ± 1.2	91.2 ± 1.9[b]	6.4 ± 1.2	3.0 ± 1.7	90.6 ± 2.0[b]
PLN	94.6 ± 1.8	0.4 ± 0.2	5.0 ± 1.8	95.4 ± 2.3	0.6 ± 0.4	4.0 ± 2.1
MLN	94.8 ± 2.9	1.0 ± 0.6	4.3 ± 2.7	96.2 ± 3.3	0.2 ± 0.2	3.6 ± 3.1
PP	98.3 ± 0.6	0.0 ± 0.0	1.8 ± 0.6	74.2 ± 17.6	0.8 ± 0.8	9.0 ± 3.0

Five NOD and five BALB/c mice were injected intravenously with anti–VCAM-1 mAb. The numbers of HEV that expressed addressin only, luminal VCAM-1 only, or both were determined by tissue section IF staining and confocal or IF microscopy. Results are expressed as mean ± SE. Mean number of HEV examined in each tissue in each mouse: BALT = 29, PLN = 182, MLN = 72, and PP = 41.

[a]Addressin = PNAd for BALT, PLN and MLN; MAdCAM-1 for PP.

[b]In each strain, the percentage of BALT HEVs with dual expression was significantly greater than the percent of PLN, MLN, and PP HEVs with dual expression ($P < 0.001$, unpaired t test). There were no differences between the two strains in the patterns of adhesion molecule expression by BALT HEVs.

amined by confocal or IF microscopy for luminal expression of VCAM-1 by HEVs.

In BALT, >90% of HEVs showed dual expression of PNAd and luminal VCAM-1 (Table I and Fig. 5, A and C); in contrast, 5% or fewer of HEVs in PLN and MLN coexpressed these molecules (Table I and Fig. 5, B and D). PE-anti–rat IgG did not stain HEVs of mice that received the negative control mAb (Fig. 5, E and F). Thus, the degree of endothelial expression of VCAM-1 clearly distinguishes HEVs in BALT from those in other secondary lymphoid tissues.

We also used immunohistochemistry to examine the expression of lymphocyte adhesion molecules in BALT, PLN, and PP of NOD, BALB/c, and C57BL/6 mice. Most lymphocytes in these tissues stained with antibodies against L-selectin, α_4, and β_7 (unpublished data). We did not note any qualitative differences in the expression of these lymphocyte adhesion molecules between strains or tissues. Our findings that BALT lymphocytes express adhesion molecules similar to those expressed by naive lymphocytes in PLN and PP suggest that many BALT lymphocytes are of naive phenotype.

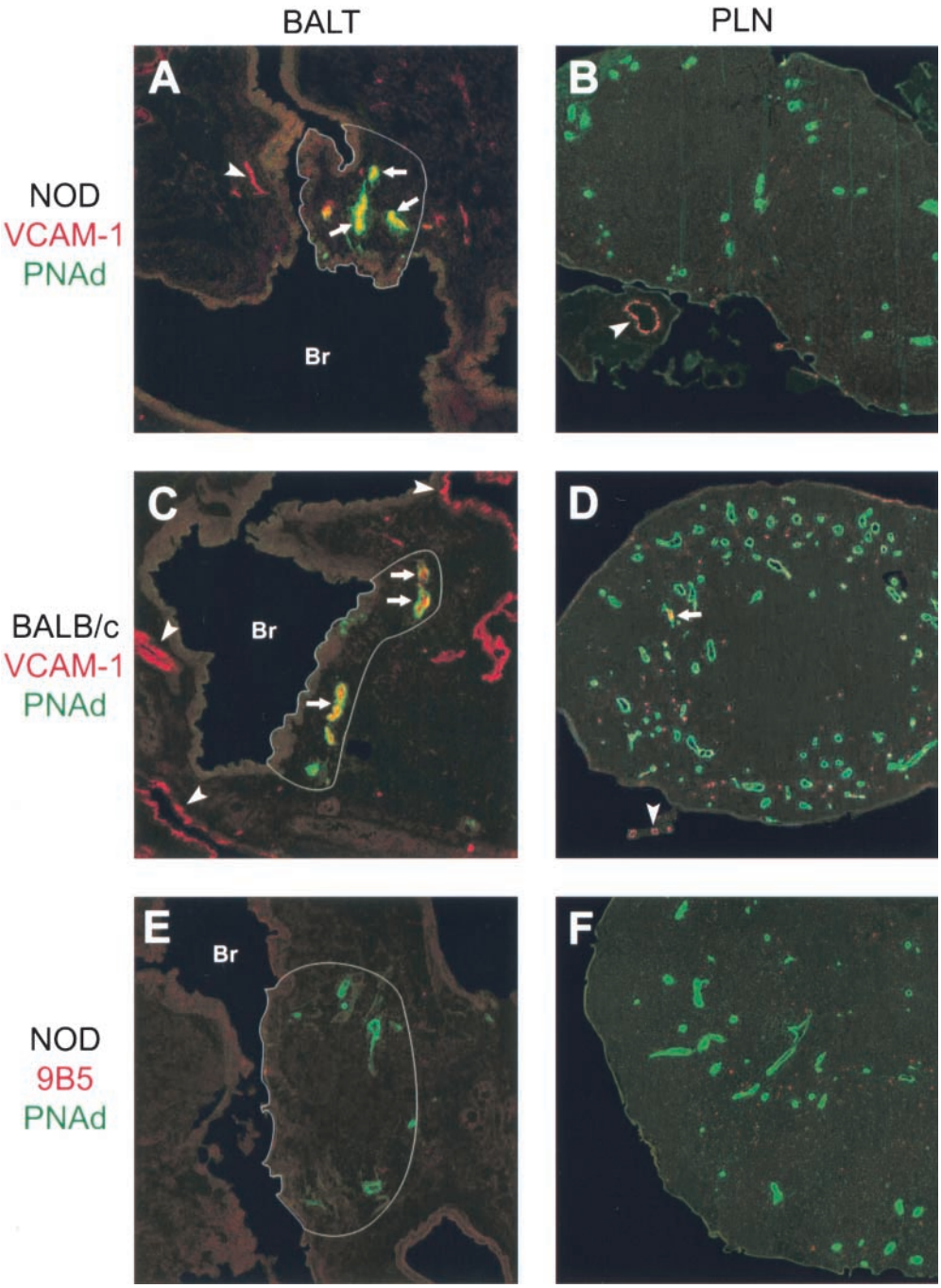

Figure 5. VCAM-1 and PNAd are coexpressed on BALT HEVs. NOD and BALB/c mice were injected intravenously with anti–VCAM-1 (A–D) or negative control (9B5) mAb (E and F). Sections of BALT (A, C, and E) and PLN (B, D, and F) were stained with PE-anti–rat IgG Ab (red) to detect injected mAb and Alexa 488–anti-PNAd mAb (green) to detect HEVs. Sections (A–D) were evaluated by confocal or IF microscopy for HEV expression of VCAM-1 and PNAd. All BALT HEVs (arrows) in NOD (A) and BALB/c (C) mice coexpress VCAM-1 and PNAd, whereas rare PLN HEVs (arrow) in NOD (B) and BALB/c (D) mice show coexpression. There is no red fluorescence on HEVs in BALT and PLN of NOD mice that were given the negative control mAb (9B5; E and F). (White line outlines BALT; arrows point to some of the HEVs that are dual positive for VCAM-1 and PNAd; arrowheads indicate VCAM-1–expressing vessels outside the lymphoid tissue; BALT original magnification = 20 [A, C, and E]; PLN original magnification = 10 [B, D, and F].)

Critical Role of the L-selectin/PNAd Pathway in Lymphocyte Homing to BALT. The strong expression of PNAd by BALT HEVs led us to hypothesize that PNAd is important in lymphocyte homing to BALT. To test this hypothesis, we used short-term in vivo lymphocyte homing assays to investigate the effects of adhesion blocking mAbs against PNAd (MECA79) and its lymphocyte ligand L-selectin (MEL-14) on homing of donor LN and spleen lymphocytes from blood into host BALT. The homing of the donor lymphocytes into BALT was strikingly reduced by MECA79 treatment compared with control mAb treatment of host mice (Fig. 6 A and Fig. 7, A and B; $P < 0.01$), and by MEL-14 treatment compared with control mAb treatment of donor lymphocytes (Fig. 6 B and Fig. 7, C and D; $P < 0.01$). As expected, both specific mAbs almost completely inhibited migration of lymphocytes into PLN, and partially inhibited migration into MLN and PP (Fig. 6, A and B). These results demonstrate that the L-selectin–PNAd pathway is critical for lymphocyte homing to BALT.

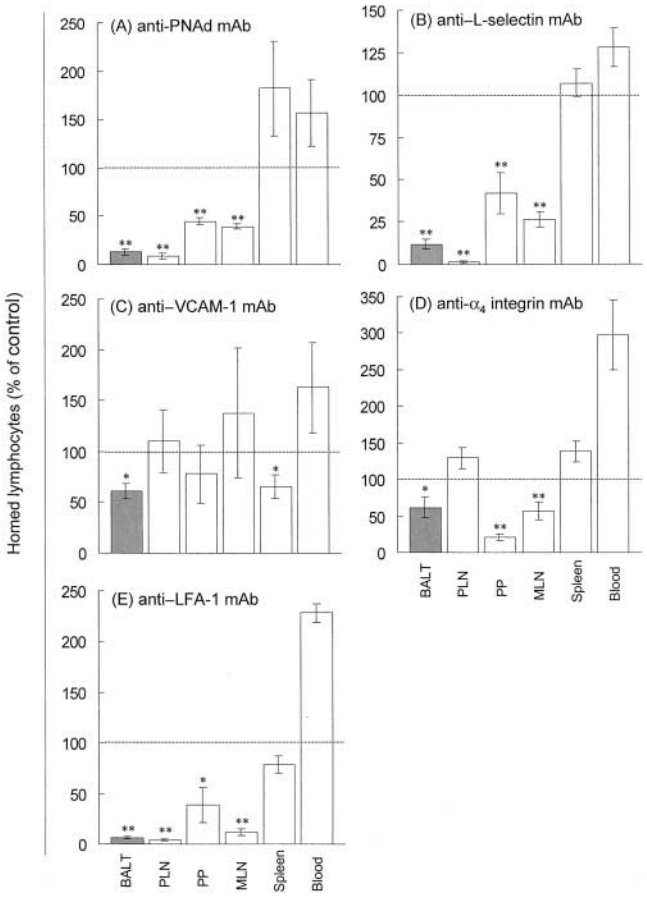

Figure 6. Antibodies to PNAd, L-selectin, VCAM-1, α_4 integrin, and LFA-1 inhibit lymphocyte homing to BALT. (A and C) TRITC-labeled mouse lymphocytes were transferred intravenously into NOD mice treated with test mAb or control mAb. (B, D, and E) TRITC-labeled mouse lymphocytes treated with test mAb or control mAb were transferred with CFSE-labeled rat internal standard lymphocytes into NOD mice. Donor cells in host lymphoid tissues were detected by flow cytometry or confocal microscopy and homing was assessed as described in Materials and Methods. Values represent the efficiency of homing compared with that of control mAb-treated cells (100%) (mean ± SE; $n = 3$ mice/group). (A) Anti-PNAd mAb almost completely blocks lymphocyte homing to BALT and PLN and partially blocks homing to PP and MLN. (B) Anti–L-selectin mAb strikingly inhibits lymphocyte homing to BALT and PLN, and partially inhibits homing to PP and MLN. Anti–VCAM-1 (C) and anti–α_4 integrin (D) mAbs partially inhibit lymphocyte homing to BALT. (E) LFA-1 is essential for lymphocyte homing to BALT. *, $P < 0.05$ and **, $P < 0.01$ compared with control mAb group.

α_4 and VCAM-1 Contribute to Lymphocyte Migration to BALT. The expression of VCAM-1 by BALT HEVs suggests that lymphocytes may migrate to BALT using $\alpha_4\beta_1$/VCAM-1 and/or $\alpha_4\beta_7$/VCAM-1 adhesion pathways. Short-term in vivo homing assays showed that anti–VCAM-1 mAb (4B12) blocked lymphocyte homing to NOD BALT by 39% (Fig. 6 C; $P < 0.05$ as compared with control mAb) and to BALB/c BALT by 44% ($P < 0.05$; not depicted), but did not significantly block homing to MLN, PLN, and PP. Similar to the anti–VCAM-1 blocking effect, anti-α_4 mAb (PS/2) blocked lymphocyte homing into NOD BALT by ~40% (Fig. 6 D; $P < 0.05$). As expected, anti-α_4 mAb blocked lymphocyte homing to PP and MLN by 80% and 40%, respectively ($P < 0.01$).

LFA-1 Is Involved in Lymphocyte Homing to BALT. Our in vivo homing assays showed that blockade of LFA-1–inhibited lymphocyte homing to BALT by 97% (Fig. 6 E, $P < 0.01$; Fig. 7, E and F). As expected, anti–LFA-1 mAb also blocked most of the lymphocyte homing to PLN, PP, and MLN (Fig. 6 E; $P < 0.01$ for PLN and MLN, $P < 0.05$ for PP). Associated with decreased migration into secondary lymphoid tissues, donor mouse lymphocyte levels were elevated in blood. These results indicate that LFA-1 is essential for lymphocyte homing to BALT.

$\alpha_4\beta_7$ Does Not Contribute to Lymphocyte Homing to BALT. The absence of staining for MAdCAM-1 on BALT HEVs suggests that lymphocyte homing to BALT does not use the $\alpha_4\beta_7$/MAdCAM-1 adhesion pathway. In in vitro experimental systems, however, $\alpha_4\beta_7$ can bind to VCAM-1 and MAdCAM-1 (6). We performed several experiments to address the potential role of $\alpha_4\beta_7$ in lymphocyte homing to BALT. First, our in vivo migration studies showed that anti-$\alpha_4\beta_7$ mAb (DATK32) had no effect on lymphocyte homing to BALT, although it significantly blocked lymphocyte homing to MLN and PP (Fig. 8 A; $P < 0.01$). Second, we found that lymphocytes from β_7 KO and WT mice migrated equally well into BALT. As expected, the β_7 integrin–deficient lymphocytes migrated poorly to PP and MLN (Fig. 8 B; $P < 0.01$). Third, to see if BALT develops normally in β_7 KO mice, we examined histologic sections of lungs from these mice. There were no significant differences in BALT area (Fig. 1) or morphology between β7 KO and WT mice (not depicted). Together, these data demonstrate that neither $\alpha_4\beta_7$/MAdCAM-1 nor $\alpha_4\beta_7$/VCAM-1 contributes to lymphocyte homing to BALT.

α_4 Integrin and VCAM-1 Recruit Memory T Cells to BALT. We wished to determine if naive T cells migrate to BALT and, if so, which adhesion pathways are involved. To do this, we used DO11.10 OVA TCR transgenic mice.

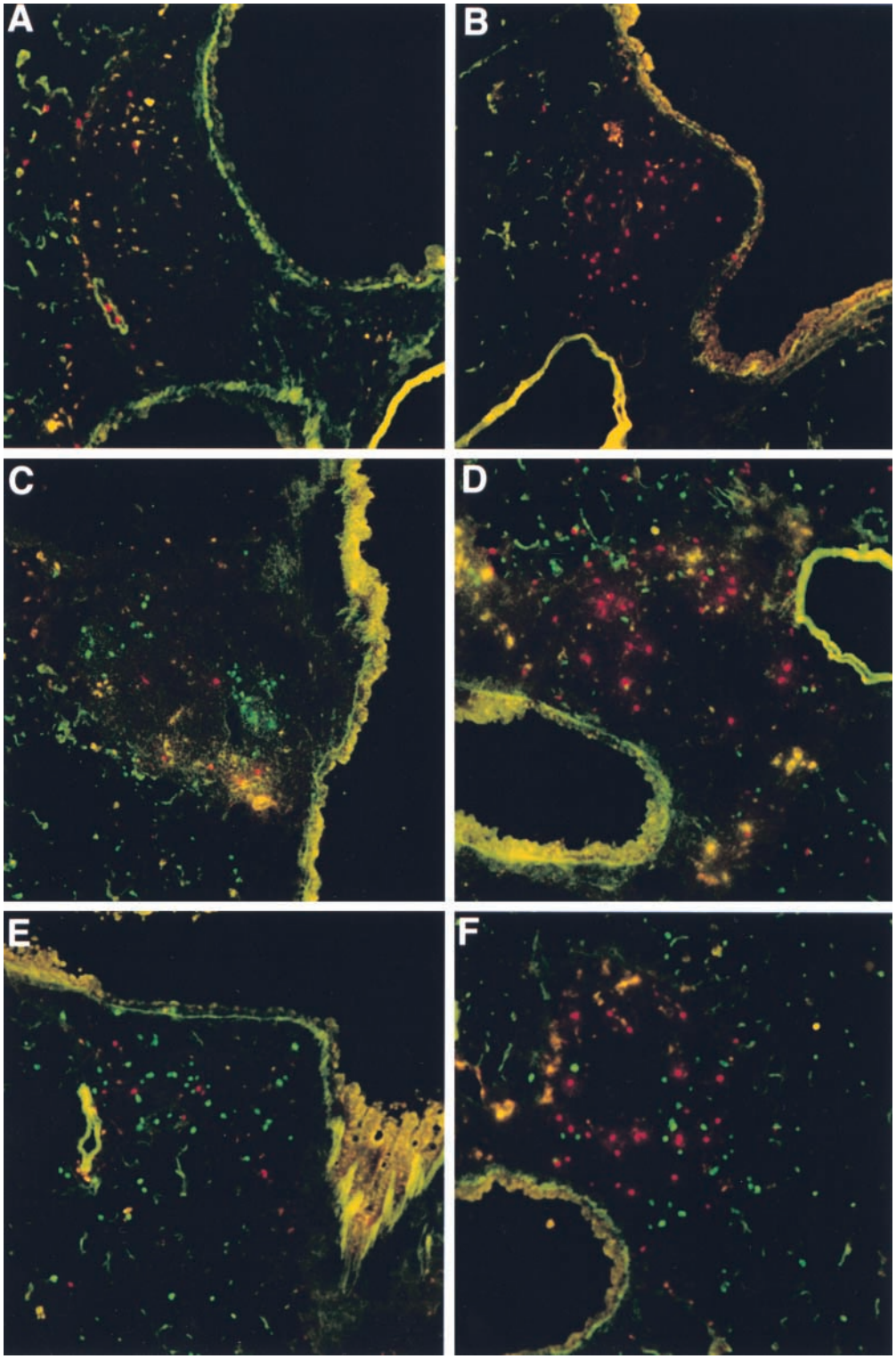

Figure 7. Anti-PNAd, L-selectin, and LFA-1 blockade of lymphocyte homing to BALT revealed by IF histology. TRITC-labeled mouse lymphocytes were transferred intravenously with or without CFSE-labeled internal standard rat lymphocytes into NOD mice. Lymphocytes that homed to BALT were observed and photographed at 40 magnification by confocal microscopy. All micrographs are two color; red and green cells are homed donor mouse and rat lymphocytes, respectively. Anti-PNAd mAb (A) inhibits donor mouse lymphocyte homing to BALT, as compared with a negative control mAb (B). Anti–L-selectin mAb (C) inhibits donor mouse lymphocyte homing to BALT, as compared with a negative control mAb (D). Anti–LFA-1 mAb (E) blocks donor mouse lymphocyte homing to BALT, as compared with a negative control mAb (F).

In young unimmunized DO11.10 mice, the T cells have a naive phenotype. Thus, when these lymphocytes are transferred into a host mouse, anti–OVA TCR mAb (KJ1–26) can be used to identify naive T cells in tissues (32). We transferred lymphocytes from 6-wk-old DO11.10 mice along with an equal number of internal standard lymphocytes (including mixed memory and naive T cells) from 6-wk-old C57BL/6 Thy1.1 mice into NOD mice. To assess homing of naive T cells to different lymphoid tissues, we compared the OVA TCR/Thy1.1 T cell ratios in each tissue with the OVA TCR/Thy1.1 T cell ratio in spleen. The ratios in BALT, LN, and PP did not differ significantly

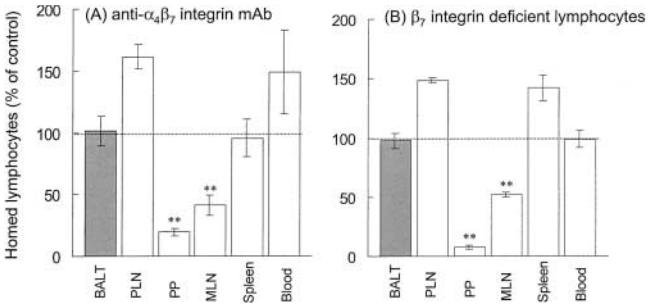

Figure 8. $\alpha_4\beta_7$ is not involved in lymphocyte homing to BALT. (A) Anti-$\alpha_4\beta_7$ mAb does not block lymphocyte homing to BALT. (B) Lymphocytes from β_7 integrin KO mice home normally to BALT. There were 3–4 mice in each group. **, $P < 0.01$ compared with control group where the value was set to 100%.

from that in spleen, indicating that BALT, like the other secondary lymphoid tissues, can efficiently recruit naive T cells from the blood (Fig. 9 A). A small but significant difference ($P < 0.05$) was observed between BALT and PP, suggesting that, relative to the OVA TCR$^+$ naive T cells, cells in the Thy 1.1$^+$ population (presumably memory T cells) migrate somewhat better to BALT than to PP.

PNAd is known to be important in the homing of naive T cells to PLN and PP, whereas the α_4–VCAM-1 pathway is thought mainly to recruit memory T cells to inflammatory sites (6). The ability of anti-α_4 and anti–VCAM-1 mAbs to partially inhibit homing of bulk populations of LN and spleen lymphocytes to BALT (Fig. 6) may result from effects on naive T cells, memory T cells, and/or B cells. Thus, we investigated the ability of anti-α_4 and anti–VCAM-1 mAbs to block the migration of B cells, naive T cells (from young DO11.10 mice), and total T cells (from old C57BL/6 mice; 80% of CD4 and CD8 cells had a CD44^{high} memory phenotype) into BALT. B cells, naive T cells, and total T cells were detected in host tissues by staining with anti-IgM^a, anti–OVA TCR, and anti-Thy 1.1 mAbs, respectively. Anti–VCAM-1 and anti-α_4 mAbs did not significantly inhibit B and naive T cell recruitment to BALT (Fig. 9 B); in contrast, anti-PNAd mAb blocked 92% of naive T cell migration to BALT (not depicted). Anti-α_4 and anti–VCAM-1 mAbs each blocked ~70% of memory T cell–rich total T cell migration to BALT (Fig. 9 B; $P < 0.01$). Anti–VCAM-1 mAb did not significantly inhibit the migration of B cells and total T cells to MLN, PLN, and PP (not depicted). Thus, α_4 and VCAM-1 are likely to recruit $\alpha_4\beta_1^+$ memory T cells to BALT, but not to LN or PP.

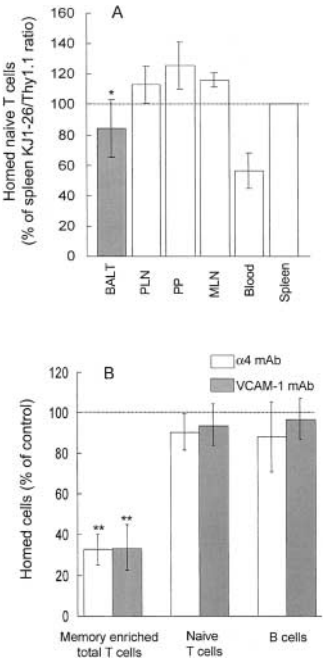

Figure 9. VCAM-1 and α_4 integrin are likely involved in memory T cell migration to BALT. (A) Naive T cells from 6-wk-old OVA TCR transgenic DO11.10 mice were transferred with equal numbers of age-matched internal standard C57BL/6 Thy1.1$^+$ lymphocytes into NOD Thy1.2$^+$ mice. Donor T cells were detected in host tissues by staining with FITC-anti–OVA TCR (clone KJ1–26) and PE–anti-Thy1.1 mAbs, followed by flow cytometry or confocal microscopy. Results are presented as the ratio of naive KJ1–26$^+$ to internal standard Thy1.1$^+$ T cells in each tissue, normalized by the ratio homed to spleen (mean ± SE). Data from three hosts show that naive T cells (OVA TCR$^+$) migrate as well as C57BL/6 T cells (a mixture of naive and memory cells) to different organs (no significant differences between spleen and BALT, PLN, PP, and MLN; *, $P < 0.05$, BALT compared with PP). (B) B and naive T cells from 6-wk-old DO11.10 mice and total T cells (80% memory phenotype) from 19-mo-old C57BL/6 Thy 1.1 mice were transferred intravenously into NOD mice. Anti-α_4 and anti–VCAM-1 mAbs inhibited the migration of memory-enriched total T cells, but not naive T cells or B cells, to BALT (**, $P < 0.01$, compared with control mAb).

Discussion

Mice as a Model for Investigation of Lymphocyte Migration to BALT. To study lymphocyte migration to BALT, it is important to use animal models with readily detectable BALT. The prominence of BALT depends on species, age, antigen stimulation, and the presence or absence of bronchopulmonary disease or systemic autoimmune disorder (8, 9, 33–36). Although guinea pigs, rabbits, and rats have well-developed BALT, the lack of immunological reagents that react with lymphocyte and endothelial adhesion molecules in these animals limits their usefulness for lymphocyte migration experiments (7, 8). In this work, we found that the presence of BALT also depends on the strain: BALT develops earlier and is more extensive in NOD than in BALB/c and C57BL/6 mice (Fig. 1). NOD mice are a model for autoimmune-mediated (type 1) diabetes and Sjogren's syndrome; these mice develop lymphoid infiltrates in pancreatic islets and several other tissues including salivary and lacrimal glands (27, 30, 37). Thus, it is possible that NOD BALT is stimulated or different from BALT in nonautoimmune-prone mice. However, we found no differences in BALT histology (except for size; Fig. 1), lymphocyte subset composition, and lymphocyte and endothelial adhesion molecule expression between NOD, BALB/c, and C57BL/6 mice.

PNAd and VCAM-1, but Not MAdCAM-1, Are Expressed by BALT HEVs. We demonstrate that BALT HEVs have a distinctive pattern of endothelial adhesion molecule expression: they are PNAd$^+$, MAdCAM-1$^-$, and VCAM-1$^+$. Moreover, we show that VCAM-1 is expressed on the endothelial luminal surface of >90% of BALT HEVs. The strong luminal expression of VCAM-1 in BALT HEVs is unique among secondary lymphoid tissues. Although VCAM-1 has been detected in association with HEVs in mouse and rat LN and PP and human tonsils, the luminal endothelial staining in these HEVs is mini-

mal compared with that of BALT HEVs (our results; 26, 31, 38).

The findings in BALT are interesting in relationship to recent papers on the expression of adhesion molecules by HEVs in other mucosal lymphoid tissues. For example, HEVs in mouse PP express MAdCAM-1, low levels of PNAd, and very little luminal VCAM-1 (our results; 22, 23, 39); HEVs in mouse nasal-associated lymphoid tissue express PNAd alone or with MAdCAM-1, but not VCAM-1 (40); HEVs in human tonsil express PNAd, but neither MAdCAM-1 nor luminal VCAM-1 (31, 41, 42); and MAdCAM-1 is not expressed on HEVs in human conjunctiva-associated lymphoid tissue (43). Thus, HEVs in mucosal lymphoid tissues at specific anatomic sites show unique patterns of adhesion molecule expression: in combination with specialized expression of chemokines and other activating factors, this may allow the selective targeting of lymphocytes to specific mucosal sites, thus enhancing the efficiency of local immune surveillance and responses.

L-selectin and PNAd Recruit Lymphocytes to BALT. In this paper, we demonstrate that anti–L-selectin and anti-PNAd mAbs almost completely inhibit homing of LN and spleen lymphocytes from blood into BALT. We also show that naive T cells migrate to BALT and that most of this migration is blocked by anti-PNAd mAb. We conclude that the specific recognition of PNAd on BALT HEVs by lymphocyte L-selectin plays a vital role in targeting lymphocytes, including naive T cells, to BALT.

$\alpha_4\beta_1$ and VCAM-1 Mediate Lymphocyte Migration to BALT. We demonstrate that VCAM-1 is expressed on the luminal surface of HEVs in BALT, at a level much higher than on HEVs in other secondary lymphoid tissues. Our in vivo migration assays show that anti-α_4 and anti–VCAM-1 mAbs inhibit ~40% of bulk lymphocyte homing to BALT, whereas anti–VCAM-1 has no significant effect on homing to PLN, PP, and MLN. We also show that neither mAb inhibits the homing of B or naive T cells to BALT. In contrast, we found that inhibition of α_4 or VCAM-1 blocks the homing of total T cells (80% memory phenotype) from old mice into BALT, suggesting that these adhesion molecules are mainly involved in the recruitment of $\alpha_4\beta_1^+$ memory T cells to BALT. Published studies indicate that $\alpha_4\beta_1$ and VCAM-1 mediate the migration of memory/effector cells to inflamed lung (11–15, 46). Thus, $\alpha_4\beta_1$/VCAM-1 may also support recruitment of bronchopulmonary memory T cells from blood into BALT, where these memory cells can meet airway antigens taken up by BALT.

Berlin-Rufenach et al. reported that VCAM-1 contributes to lymphocyte homing to LN (26). Consistent with our work, however, their published histology shows predominantly abluminal staining for VCAM-1 on LN HEVs. Moreover, they and others found that anti–VCAM-1 mAbs did not inhibit homing of lymphocytes to LN and PP (our results; 22, 44, 45) unless LFA-1 was absent or blocked (26). Thus, a functional role for VCAM-1 in lymphocyte migration to LN and PP could only be revealed when the dominant LFA-1 pathway was inhibited or missing. In contrast to LN and PP, we find that lymphocyte homing to BALT involves α_4 and VCAM-1, but not $\alpha_4\beta_7$, and is easily detectable in standard in vivo homing assays. These findings indicate that $\alpha_4\beta_1$ and VCAM-1 contribute much more prominently in lymphocyte homing to BALT than to other secondary lymphoid tissues.

$\alpha_4\beta_7$ and MAdCAM-1 Are Not Required for Lymphocyte Homing to BALT. In this work, we found that: a) MAdCAM-1 is not expressed by BALT HEVs; b) $\alpha_4\beta_7$ is not required for migration of lymphocytes into BALT; and c) BALT in WT mice is histologically indistinguishable from BALT in β_7 KO mice. These results indicate that the $\alpha_4\beta_7$/MAdCAM-1 adhesion system is not involved in lymphocyte migration into BALT. Thus, the $\alpha_4\beta_7$/MAdCAM-1 pathway is not required for lymphocyte homing to all mucosal secondary lymphoid tissues; instead, its involvement and that of $\alpha_4\beta_1$/VCAM-1 help distinguish the mechanisms of lymphocyte migration to specific mucosal sites.

LFA-1 Is Essential for Lymphocyte Homing to BALT. We found that anti–LFA-1 mAb almost completely blocks lymphocyte homing to BALT and LN, and partially blocks homing to PP. This is in agreement with previous studies showing that LFA-1 is essential for activation-dependent adhesion of lymphocytes to PLN and PP HEVs (3, 5, 24–26). It is likely that LFA-1 mediates lymphocyte homing to BALT through similar mechanisms.

Multistep Cascades for Lymphocyte Homing to PP and BALT. Lymphocyte migration from blood into secondary lymphoid tissues is not a random process; it is controlled by highly specific interactions between lymphocytes and HEV endothelial cells in these tissues. These interactions consist of multistep cascades with at least four sequential adhesion and activation steps, including lymphocyte tethering and rolling (step 1); lymphocyte activation by chemokines or other activating molecules (step 2); activation dependent arrest or firm adhesion (step 3); and diapedesis into tissues (step 4). The adhesion cascades that govern the migration of naive lymphocytes into PLN and PP have been defined by in situ microscopy studies (3, 5). The data from our paper suggest that the adhesion cascades in BALT may parallel those in PP, but with $\alpha_4\beta_1$/VCAM-1 interaction in BALT serving the role of $\alpha_4\beta_7$/MAdCAM-1 interaction in PP.

In PP HEVs, lymphocytes tether and roll (step 1) by lymphocyte L-selectin binding to carbohydrate epitopes on endothelial MAdCAM-1 and by lymphocyte $\alpha_4\beta_7$ binding to MAdCAM-1 (3, 47). The chemokine/chemokine receptor pairs CCL21 (SLC/6Ckine)/CCR7 and CXCL12 (SDF-1)/CXCR4 are involved in lymphocyte activation (step 2; references 48–51). Firm adhesion of lymphocytes to the endothelium is mediated by $\alpha_4\beta_7$/MAdCAM-1 and LFA-1 (step 3; reference 3). The molecules that mediate diapedesis (step 4) into the PP include CXCL13 (BLC) and its receptor CXCR5 (49).

By analogy with these events in PP, our results suggest a model in which lymphocytes tether and roll on BALT HEVs by lymphocyte L-selectin binding to carbohydrate epitopes on endothelial PNAd and by lymphocyte $\alpha_4\beta_1$

binding to VCAM-1 (step 1). $\alpha_4\beta_1$/VCAM-1 interactions may slow rolling cells, which arrest on BALT endothelium through activation-dependent $\alpha_4\beta_1$/VCAM-1 and LFA-1–mediated firm adhesion (step 3). The molecules that mediate lymphocyte activation (step 2) and diapedesis into BALT (step 4) remain to be defined.

In BALT as in PP, specific lymphocyte subsets may be able to migrate into tissue using only some of the adhesion molecules that are available in their cascade. For example, memory T cells might tether and roll (step 1) on BALT HEVs using $\alpha_4\beta_1$ and VCAM-1, instead of L-selectin and PNAd. Thus, by analogy to the efficient homing of $\alpha_4\beta_7^+$ memory T cells through MAdCAM-1$^+$ HEVs in PP, the availability of VCAM-1 on BALT HEVs may be important in recruitment of $\alpha_4\beta_1^+$ memory T cells into BALT. In contrast, we found that anti-PNAd mAb, but not mAbs against α_4 and VCAM-1, blocks migration of naive T cells into BALT. This suggests that these naive cells may be able to tether and roll on HEVs without using $\alpha_4\beta_1$ and VCAM-1, instead relying on lymphocyte L-selectin binding to the PNAd that is highly expressed on BALT HEVs.

Potential Significance of BALT in Pulmonary Immune Responses. Striking similarities between BALT and PP support the concept that these tissues have parallel physiologic and pathologic roles in pulmonary and intestinal immunity, respectively (7). The epithelial surface over PP contains M cells that mediate the transport of antigens from the intestinal lumen into PP. PPs also support the migration of naive T and B lymphocytes from the blood via HEV. Thus, PPs provide a microenvironment for activation and initial differentiation of naive lymphocytes responding to intestinal antigens. After further maturation in the MLN, the lymphocytes enter the systemic circulation, where they comprise a population of $\alpha_4\beta_7^+$ memory cells that display selective, efficient migration to intestinal sites such as PP and lamina propria (6). Adhesion cascades, in which $\alpha_4\beta_7$ and MAdCAM-1 play prominent tissue-selective roles, mediate this homing of lymphocytes to intestine. Thus, $\alpha_4\beta_7$ and MAdCAM-1 unify lymphocyte migration to intestinal secondary lymphoid tissues (PP) and effector sites (lamina propria; references 3, 16, 22).

BALT is thought to function as the primary site for presentation of airway antigens to the immune system. Here, we show that BALT HEVs support the migration of naive T cells from blood into BALT, where these lymphocytes can encounter antigens that have been transported from the airway lumen by bronchial M cells. After maturation in BALT and/or bronchial LN, these lymphocytes could enter the bloodstream, where they would comprise a recirculating population of $\alpha_4\beta_1^+$ memory cells for respiratory tract antigens. These memory lymphocytes would migrate efficiently from blood into BALT and other bronchopulmonary tissues using adhesion cascades in which $\alpha_4\beta_1$ and VCAM-1 contribute prominently to tissue selectivity. Thus, $\alpha_4\beta_1$ and VCAM-1 may help unify lymphocyte migration to bronchopulmonary secondary lymphoid tissues (BALT) and effector sites (lung).

In conclusion, we found that most BALT HEVs coordinately express the endothelial adhesion molecules PNAd and VCAM-1, the latter at a level not seen on HEVs in other secondary lymphoid tissues. Moreover, lymphocyte homing to BALT involves prominent participation of L-selectin/PNAd, $\alpha_4\beta_1$/VCAM-1, and LFA-1 adhesion pathways. We propose that these receptor/ligand pairs participate in a specialized adhesion cascade that regulates the interactions of circulating lymphocytes with BALT HEVs, and that allows the targeting of naive and memory T cells to these airway secondary lymphoid tissues. The shared participation of $\alpha_4\beta_1$/VCAM-1 in BALT and in pulmonary parenchymal recruitment of lymphocytes provides a mechanism to unite migration pathways, and thus immune responses, in BALT and lung.

We thank C. Tudor for help with photography, A. Benson for administrative support, J. Jang, J. Twelves, and E. Resurreccion for assistance with mAb preparation and immunohistochemical staining, Dr. B. Engelhardt for anti–VCAM-1 mAbs, Drs. D. Loh and O. Kanagawa for DO11.10 mice, and Dr. J. Kappler for KJ1–26 mAb. We also thank Drs. D. Campbell, B. Engelhardt, R. Ettinger, E. Kunkel, A. Mennis-Mikulowska, and J. Pan for discussing this work and critically reading the manuscript.

This work was supported by grants from the National Institutes of Health (R21 AI47574) and the Department of Veterans Affairs Office of Research and Development given to E.C. Butcher and S.A. Michie, a grant from the Deutsche Forschungsgemeinschaft (WA1127/1-3) given to N. Wagner, and a grant from the Ministry of Education, Culture, Sports, Science and Technology, Japan (C2-13670339) given to B. Xu.

Submitted: 23 April 2001
Revised: 27 February 2003
Accepted: 17 March 2003

References

1. Butcher, E.C., and L.J. Picker. 1996. Lymphocyte homing and homeostasis. *Science*. 272:60–66.
2. Butcher, E.C. 1991. Leukocyte-endothelial cell recognition: three (or more) steps to specificity and diversity. *Cell*. 67: 1033–1036.
3. Bargatze, R.F., M.A. Jutila, and E.C. Butcher. 1995. Distinct roles of L-selectin and integrins alpha 4 beta 7 and LFA-1 in lymphocyte homing to Peyer's patch-HEV in situ: the multistep model confirmed and refined. *Immunity*. 3:99–108.
4. Springer, T.A. 1995. Traffic signals on endothelium for lymphocyte recirculation and leukocyte emigration. *Annu. Rev. Physiol*. 57:827–872.
5. Warnock, R.A., S. Askari, E.C. Butcher, and U.H. von Andrian. 1998. Molecular mechanisms of lymphocyte homing to peripheral lymph nodes. *J. Exp. Med*. 187:205–216.
6. Butcher, E.C., M. Williams, K. Youngman, L. Rott, and M. Briskin. 1999. Lymphocyte trafficking and regional immunity. *Adv. Immunol*. 72:209–253.
7. Bienenstock, J., N. Johnston, and D.Y.E. Perey. 1973. Bronchial lymphoid tissue. I. Morphologic characteristics. *Lab. Invest*. 28:686–692.
8. Pabst, R., and I. Gehrke. 1990. Is the bronchus-associated lymphoid tissue (BALT) an integral structure of the lung in normal mammals, including humans? *Am. J. Respir. Cell Mol.*

Biol. 3:131–135.
9. Sminia, T., G.J. van der Brugge-Gamelkoorn, and S.H.M. Jeurissen. 1989. Structure and function of bronchus-associated lymphoid tissue (BALT). *Crit. Rev. Immunol.* 9:119–150.
10. van der Brugge-Gamelkoorn, G.J., and G. Kraal. 1985. The specificity of the high endothelial venule in bronchus-associated lymphoid tissue (BALT). *J. Immunol.* 134:3746–3750.
11. Wolber, F.M., J.L. Curtis, A.M. Milik, T. Fields, G.D. Seitzman, K. Kim, S. Kim, J. Sonstein, and L.M. Stoolman. 1997. Lymphocyte recruitment and the kinetics of adhesion receptor expression during the pulmonary immune response to particulate antigen. *Am. J. Pathol.* 151:1715–1727.
12. Wolber, F.M., J.L. Curtis, P. Maly, R.J. Kelly, P. Smith, T.A. Yednock, J.B. Lowe, and L.M. Stoolman. 1998. Endothelial selectins and alpha4 integrins regulate independent pathways of T lymphocyte recruitment in the pulmonary immune response. *J. Immunol.* 161:4396–4403.
13. Chin, J.E., C.A. Hatfield, G.E. Winterrowd, J.R. Brashler, S.L. Vonderfecht, S.F. Fidler, R.L. Griffin, K.P. Kolbasa, R.F. Krzesicki, L.M. Sly, et al. 1997. Airway recruitment of leukocytes in mice is dependent on alpha4- integrins and vascular cell adhesion molecule-1. *Am. J. Physiol.* 272:L219–L229.
14. Feng, C.G., W.J. Britton, U. Palendira, N.L. Groat, H. Briscoe, and A.G. Bean. 2000. Up-regulation of VCAM-1 and differential expansion of beta integrin-expressing T lymphocytes are associated with immunity to pulmonary Mycobacterium tuberculosis infection. *J. Immunol.* 164:4853–4860.
15. Nakajima, H., H. Sano, T. Nishimura, S. Yoshida, and I. Iwamoto. 1994. Role of vascular cell adhesion molecule 1/very late activation antigen 4 and intercellular adhesion molecule 1/lymphocyte function-associated antigen 1 interactions in antigen-induced eosinophil and T cell recruitment into the tissue. *J. Exp. Med.* 179:1145–1154.
16. Wagner, N., J. Lohler, E.J. Kunkel, K. Ley, E. Leung, G. Krissansen, K. Rajewsky, and W. Muller. 1996. Critical role for beta7 integrins in formation of the gut-associated lymphoid tissue. *Nature.* 382:366–370.
17. Johnson, G.G., A. Mikulowska, E.C. Butcher, L.M. McEvoy, and S.A. Michie. 1999. Anti-CD43 monoclonal antibody L11 blocks migration of T cells to inflamed pancreatic islets and prevents development of diabetes in nonobese diabetic mice. *J. Immunol.* 163:5678–5685.
18. Engelhardt, B., M.T. Martin-Simonet, L.S. Rott, E.C. Butcher, and S.A. Michie. 1998. Adhesion molecule phenotype of T lymphocytes in inflamed CNS. *J. Neuroimmunol.* 84:92–104.
19. Butcher, E.C., R.G. Scollay, and I.L. Weissman. 1980. Direct fluorescent labeling of cells with fluorescein or rhodamine isothiocyanate. II. Potential application to studies of lymphocyte migration and maturation. *J. Immunol. Methods.* 37:109–121.
20. Lyons, A.B., and C.R. Parish. 1994. Determination of lymphocyte division by flow cytometry. *J. Immunol. Methods.* 171:131–137.
21. Streeter, P.R., B.T. Rouse, and E.C. Butcher. 1988. Immunohistologic and functional characterization of a vascular addressin involved in lymphocyte homing into peripheral lymph nodes. *J. Cell Biol.* 107:1853–1862.
22. Hamann, A., D.P. Andrew, D. Jablonski-Westrich, B. Holzmann, and E.C. Butcher. 1994. Role of alpha 4-integrins in lymphocyte homing to mucosal tissues in vivo. *J. Immunol.* 152:3282–3293.
23. Streeter, P., E. Berg, B. Rouse, F. Bargatze, and C. Butcher. 1988. A tissue-specific endothelial cell molecule involved in lymphocyte homing. *Nature.* 331:41–46.
24. Hamann, A., D. Jablonski-Westrich, A. Duijvestijn, E.C. Butcher, H. Baisch, R. Harder, and H.G. Thiele. 1988. Evidence for an accessory role of LFA-1 in lymphocyte-high endothelium interaction during homing. *J. Immunol.* 140:693–699.
25. Andrew, D.P., J.P. Spellberg, H. Takimoto, R. Schmits, T.W. Mak, and M.M. Zukowski. 1998. Transendothelial migration and trafficking of leukocytes in LFA-1-deficient mice. *Eur. J. Immunol.* 28:1959–1969.
26. Berlin-Rufenach, C., F. Otto, M. Mathies, J. Westermann, M.J. Owen, A. Hamann, and N. Hogg. 1999. Lymphocyte migration in lymphocyte function–associated antigen (LFA)-1–deficient mice. *J. Exp. Med.* 189:1467–1478.
27. Mikulowski-Mennis, A., B. Xu, J.M. Berberian, and S.A. Michie. 2001. Lymphocyte migration to inflamed lacrimal glands is mediated by vascular cell adhesion molecule-1/alpha4beta1 integrin, peripheral node addressin/L-selectin, and lymphocyte function-associated antigen-1 adhesion pathways. *Am. J. Pathol.* 159:671–681.
28. Steffen, B.J., E.C. Butcher, and B. Engelhardt. 1994. Evidence for involvement of ICAM-1 and VCAM-1 in lymphocyte interaction with endothelium in experimental autoimmune encephalomyelitis in the central nervous system in the SJL/J mouse. *Am. J. Pathol.* 145:189–201.
29. Vajkoczy, P., M. Laschinger, and B. Engelhardt. 2001. Alpha4-integrin-VCAM-1 binding mediates G protein-independent capture of encephalitogenic T cell blasts to CNS white matter microvessels. *J. Clin. Invest.* 108:557–565.
30. Yang, X.D., S.A. Michie, R. Tisch, N. Karin, L. Steinman, and H.O. McDevitt. 1994. A predominant role of a4 integrin in the spontaneous development of autoimmune diabetes in nonobese diabetic mice. *Proc. Natl. Acad. Sci. USA.* 91: 12604–12608.
31. Perry, M.E., W.N. Kirkpatrick, L.C. Happerfield, and M.J. Gleeson. 1996. Expression of adhesion molecules on the microvasculature of the pharyngeal tonsil (adenoid). *Acta Otolaryngol. Suppl.* 523:47–51.
32. Murphy, K.M., A.B. Heimberger, and D.Y. Loh. 1990. Induction by antigen of intrathymic apoptosis of CD4+ CD8+TCRlo thymocytes in vivo. *Science.* 250:1720–1723.
33. Sato, A., K. Chida, M. Iwata, and H. Hayakawa. 1992. Study of bronchus-associated lymphoid tissue in patients with diffuse panbronchiolitis. *Am. Rev. Respir. Dis.* 146:473–478.
34. Sato, A., H. Hayakawa, H. Uchiyama, and K. Chida. 1996. Cellular distribution of bronchus-associated lymphoid tissue in rheumatoid arthritis. *Am. J. Respir. Crit. Care Med.* 154: 1903–1907.
35. Suda, T., K. Chida, H. Hayakawa, S. Imokawa, M. Iwata, H. Nakamura, and A. Sato. 1999. Development of bronchus-associated lymphoid tissue in chronic hypersensitivity pneumonitis. *Chest.* 115:357–363.
36. Brodie, S.J., C. de la Rosa, J.G. Howe, J. Crouch, W.D. Travis, and K. Diem. 1999. Pediatric AIDS-associated lymphocytic interstitial pneumonia and pulmonary arterio-occlusive disease: role of VCAM-1/VLA-4 adhesion pathway and human herpesviruses. *Am. J. Pathol.* 154:1453–1464.
37. Hanninen, A., C. Taylor, P.R. Streeter, L.S. Stark, J.M. Sarte, J.A. Shizuru, O. Simell, and S.A. Michie. 1993. Vascular addressins are induced on islet vessels during insulitis in

nonobese diabetic mice and are involved in lymphoid cell binding to islet endothelium. *J. Clin. Invest.* 92:2509–2515.
38. May, M.J., G. Entwistle, M.J. Humphries, and A. Ager. 1993. VCAM-1 is a CS1 peptide-inhibitable adhesion molecule expressed by lymph node high endothelium. *J. Cell Sci.* 106:109–119.
39. Streeter, P.R., B.T.N. Rouse, and E.C. Butcher. 1988. Immunohistologic and functional characterization of a vascular addressin involved in lymphocyte homing into peripheral lymph nodes. *J. Cell Biol.* 107:1853–1862.
40. Csencsits, K.L., M.A. Jutila, and D.W. Pascual. 1999. Nasal-associated lymphoid tissue: phenotypic and functional evidence for the primary role of peripheral node addressin in naive lymphocyte adhesion to high endothelial venules in a mucosal site. *J. Immunol.* 163:1382–1389.
41. Michie, S.A., P.R. Streeter, P.A. Bolt, E.C. Butcher, and L.J. Picker. 1993. The human peripheral lymph node vascular addressin. An inducible endothelial antigen involved in lymphocyte homing. *Am. J. Pathol.* 143:1688–1698.
42. Briskin, M., D. Winsor-Hines, A. Shyjan, N. Cochran, S. Bloom, J. Wilson, L.M. McEvoy, E.C. Butcher, N. Kassam, C.R. Mackay, et al. 1997. Human mucosal addressin cell adhesion molecule-1 is preferentially expressed in intestinal tract and associated lymphoid tissue. *Am. J. Pathol.* 151:97–110.
43. Haynes, R.J., P.J. Tighe, R.A. Scott, and H. Singh Dua. 1999. Human conjunctiva contain high endothelial venules that express lymphocyte homing receptors. *Exp. Eye Res.* 69: 397–403.
44. Leuker, C.E., M. Labow, W. Muller, and N. Wagner. 2001. Neonatally induced inactivation of the vascular cell adhesion molecule 1 gene impairs B cell localization and T cell–dependent humoral immune response. *J. Exp. Med.* 193: 755–767.
45. Koni, P.A., S.K. Joshi, U.-A. Temann, D. Olson, L. Burkly, and R.A. Flavell. 2001. Conditional vascular cell adhesion molecule 1 deletion in mice: impaired lymphocyte migration to bone marrow. *J. Exp. Med.* 193:741–753.
46. Tietz, W., and A. Hamann. 1997. The migratory behavior of murine CD4+ cells of memory phenotype. *Eur. J. Immunol.* 27:2225–2232.
47. Berlin, C., R.F. Bargatze, J.J. Campbell, U.H. von Andrian, M.C. Szabo, S.R. Hasslen, R.D. Nelson, E.L. Berg, S.L. Erlandsen, and E.C. Butcher. 1995. Alpha 4 integrins mediate lymphocyte attachment and rolling under physiologic flow. *Cell.* 80:413–422.
48. Gunn, M.D., K. Tangemann, C. Tam, J.G. Cyster, S.D. Rosen, and L.T. Williams. 1998. A chemokine expressed in lymphoid high endothelial venules promotes the adhesion and chemotaxis of naive T lymphocytes. *Proc. Natl. Acad. Sci. USA.* 95:258–263.
49. Okada, T., V.N. Ngo, E.H. Ekland, R. Forster, M. Lipp, D.R. Littman, and J.G. Cyster. 2002. Chemokine requirements for B cell entry to lymph nodes and Peyer's patches. *J. Exp. Med.* 196:65–75.
50. Stein, J.V., A. Rot, Y. Luo, M. Narasimhaswamy, H. Nakano, M.D. Gunn, A. Matsuzawa, E.J. Quackenbush, M.E. Dorf, and U.H. von Andrian. 2000. The CC chemokine thymus-derived chemotactic agent 4 (TCA-4, secondary lymphoid tissue chemokine, 6Ckine, exodus-2) triggers lymphocyte function–associated antigen 1–mediated arrest of rolling T lymphocytes in peripheral lymph node high endothelial venules. *J. Exp. Med.* 191:61–76.
51. Warnock, R.A., J.J. Campbell, M.E. Dorf, A. Matsuzawa, L.M. McEvoy, and E.C. Butcher. 2000. The role of chemokines in the microenvironmental control of T versus B cell arrest in Peyer's patch high endothelial venules. *J. Exp. Med.* 191:77–88.